Journal Pre-proof

Wireless water quality monitoring and spatial mapping with disposable whole-copper electrochemical sensors and a smartphone

Jianjun Liao, Feng Chang, Xiaohu Han, Chengjun Ge, Shiwei Lin

Please cite this article as: Liao J, Chang F, Han X, Ge C, Lin S, Wireless water quality monitoring and spatial mapping with disposable whole-copper electrochemical sensors and a smartphone, *Sensors and Actuators: B. Chemical* (2019), doi: https://doi.org/10.1016/j.snb.2019.127557

Wireless water quality monitoring and spatial mapping with disposable whole-copper electrochemical sensors and a smartphone

Jianjun Liao[a,b], Feng Chang[c], Xiaohu Han[c], Chengjun Ge[b,d], Shiwei Lin[a,e,*]

[a] State Key Laboratory of Marine Resource Utilization in South China Sea, Hainan University, Haikou 570228, China

[b] College of Ecology and Environment, Hainan University, Haikou 570228, China

[c] College of Applied Science and Technology, Hainan University, Danzhou 571737, China

[d] College of Life Sciences, Zhejiang University, Hangzhou, Zhejiang, 310058, China

[e] College of Materials Science and Engineering, Hainan University, Haikou 570228, China

[*] Address correspondence to: linsw@hainanu.edu.cn   (S. Lin)

Graphical abstract

Highlights

- A smartphone-based water quality monitoring system was successfully constructed.

- It comprised of a whole-copper electrochemical sensor, a hand-held detector, a smartphone, and a Cloud map website.

- The hand-held detector can perform CA, SWV, and LSV methods.

- The detection of Pb^{2+} ions and COD was realized by the smartphone-based system.

- Spatiotemporal mapping of water contamination was displayed on the central website.

Abstract

Portable, rapid, and cost-effective detection of environmental contamination remains an important challenge in the field of water quality analysis. Herein, we described a smartphone-based water quality monitoring system that allowed for the quantification of Pb^{2+} ions and chemical oxygen demand (COD) at an exact location. The system was composed of four main parts: (i) a whole-copper electrochemical sensor, (ii) a hand-held detector, (iii) a smartphone installed with a custom application program, and (iv) a Cloud map website. The sensor chips were made of low-cost copper, including microfabricated Cu working electrodes, Cu counter electrodes, and $Cu/CuCl_2$ reference electrodes. The hand-held detector (~50 g) can perform several types of electroanalytical techniques, including chronoamperometry, cyclic voltammetry, linear sweep voltammetry, and square wave voltammetry. With an Application (App), the smartphone was used to control the detector and visualize the testing results in real time. A Cloud map website was used to receive and display the contamination concentrations and geographic locations for public sharing and viewing. Since the smartphone-based system is cost-effective, small in size, field-portable, and fully wireless, it shows great potential for applications in resource-limited settings.

Keywords: Smartphone, Whole-copper electrochemical sensors; Cloud service; Water quality

1. Introduction

With the rapid development of industry throughout the world, various chemical substances have been released into the water body, many of which may cause significant threats to human health and the ecosystem. For example, lead (Pb) can damage human tissues and organs even at low concentrations, and thus has been acknowledged to be a human carcinogen by the World Health Organization (WHO) [1,2]. Chemical oxygen demand (COD) is regarded as a critical index related to the total pollution load of the water body and strictly controlled by the environmental regulatory agencies [3,4]. However, most routine water analytical methods suffer from bulky and expensive instruments, complex laboratory operations, and skilled technical personnel [5-8]. These problems have become a challenge in the field of water quality monitoring, especially in remote, low-resource, and undereducated areas.

Currently, electrochemical analysis methods have received widespread attention due to the properties such as high sensitivity, simple operation, and rapid analysis. Electrochemical analyzer/workstation is a standard instrument for the electrochemical analysis. However, traditional electrochemical analyzers/workstations are expensive, bulky, and not well-suited for on-site detection. The smartphone provides new opportunities for the development of next-generation portable electrochemical systems. First, the smartphone has a vast user community. According to Newzoo's global mobile market report (2018), there were 3.0 billion smartphone users globally at the end of 2018, and this number will hit 3.8 billion by 2021[9]. Second, the smartphone is similar to a mini-computer with great built-in functions, such as user-friendly operating systems, convenient touch-screen displays, strong central processors, and ample data storage. Therefore, the electrochemical analyzer/workstation coupled with smartphone can significantly simplify the electronic design, reduce volume, and decrease the cost of the system. This is because

some hardware modules initially designed in the electrical reader, like input button, signal conditioning, and screen display, can be realized by the software design in the smartphone. Inspired by these advantages, smartphone-based electrochemical analyzers (SBEAs) have obtained great achievements in the field of point-of-care testing and mobile diagnostics [10-15].

Screen-printed electrodes (SPEs) are an essential component in electroanalysis [16-21]. However, most SPEs are fabricated by gold, silver, or carbon ink. From the cost and fabrication perspectives, these electrodes are not ideal. For example, the viscosity of the paste should be modulated before their printing on the substrate, and different curing temperatures are needed according to the type of inks. Recently, whole-copper electrochemical sensor (WCES) chips provided a viable option in disposable sensor applications [22-24]. The WCES chips were fully fabricated by a low-cost copper, including the Cu working electrode (WE), Cu counter electrode (CE), and $Cu/CuCl_2$ reference electrode (RE). However, the WCES chips shows the high overpotential and poor selectivity, and the fabrication of WCES chips is primarily performed in a cleanroom. Expensive cleanroom instruments are needed during the fabrication. Besides, the fabrication procedures, including metal deposition, photolithography, and lift-off, are time-consuming and cost-prohibitive [25-28]. Therefore, we proposed a simple, efficient, and cleanroom-free method for the fabrication of WCES chips (Figure S1). Furthermore, Cu nanoflowers were electrodeposited onto WCES to decrease the overpotential and increase the selectivity.

Additionally, the supporting electrolyte plays a vital role in the electrochemical water analysis, but it is often overlooked in most current works [2, 29-32]. The proper selection of the supporting electrolyte can realize the detection of different water quality indices. The Papautsky group has demonstrated the feasibility of detecting heavy metal ions in acetate buffer solution using Cu electrodes[23]. The acetate buffer was chosen primarily because the acidic medium is beneficial for the ionization of heavy metal ions [33,34], which can enhance the measurement accuracy. It should be noted that Cu electrodes also show good electrocatalytic activity to organic

compounds in alkaline medium, and the magnitude of oxidation current reflects the COD level in water samples [3,35,36]. Therefore, multiplexed water quality analysis can be achieved by the proper selection of supporting electrolyte. However, to the best of our knowledge, there are few reports on the effect of the supporting electrolyte [37-39].

In this paper, a smartphone-based water quality monitoring system was proposed for the detection of Pb^{2+} ions and COD. As shown in Figure 1a, the system was composed of four main parts: (i) a whole-copper electrochemical sensor, (ii) a hand-held detector, (iii) a smartphone equipped with an application program, and (iv) a Cloud map website. The hand-held detector was used to perform electrochemical measurements on WCES and transmit the measured data to the smartphone via Bluetooth. The smartphone was used to control the system, process data, and display results in real time through a customized Android application (App). Additionally, the operators can upload the sample-related information, including the measured results, dates, and GPS coordinates of the testing sites, to the Cloud map website through 3G or 4G networks. The website is available for all registered users worldwide, and they can share their testing results to the public. We believe that such a collaborative mapping approach has enormous potential for improving water pollution.

2. Experimental section

2.1 Chemical reagents

All reagents were purchased from Aladdin Reagent Co. Ltd. and used without further purification. 0.1 M acetate buffer (pH = 5) was chosen as the acidic supporting electrolyte. 0.05 M NaOH (pH = 10) was chosen as the alkaline supporting electrolyte. Pb^{2+} stock solutions were prepared by dissolving various concentrations of $Pb(NO_3)_2$ in 0.1 M acetate buffer. COD standard substances were prepared by dissolving various concentrations of glucose in 0.05 M NaOH.

2.2 Fabrication of the whole-copper electrochemical sensors

The whole-copper electrochemical sensors were prepared by the thermal transfer printing method, which is a low-cost and efficient technique for the manufacturing of printed circuit boards. Using this method, a simple laser printer and thermal transfer machine were sufficient for the fabrication of the sensor chips. The fabrication process was illustrated in Figure S1 (Supporting Information).

2.3 Design of a hand-held detector

The hand-held detector was used to perform the electrochemical measurements, record the measured data, and send it to the smartphone. Figure 1b shows the schematic diagram of the detector. The microcontroller unit (MCU, STM32F103RCT6) was chosen because it contains a 32-bit ARM processor, $3 \times$ 12-bit A/D converters, and 2×12-bit D/A converters. The generation of the excitation signal and the conversion of the analog signal into a digital signal can be accomplished on the same MCU, thereby significantly decreasing the manufacturing cost. The potentiostat module was a critical component in the electrical circuit, which consisted of two operational amplifiers in AD8608. Another two operational amplifiers in AD8608 were used as the low-pass filter to decrease the circuit noise. A Bluetooth module (HC-06) was used to transfer the data and command.

2.4 Design of a smartphone-based water quality monitoring system

As shown in Figure 1a, the smartphone-based water quality monitoring system consisted of a WCES chip, a hand-held detector, a smartphone, and a Cloud map website. WCES chip was plugged into the socket of the hand-held detector, and the detector was connected to the smartphone via Bluetooth. The hand-held detector can perform four types of detection techniques: chronoamperometry (CA), cyclic voltammetry (CV), linear sweep voltammetry (LSV), and square wave voltammetry (SWV). The user input the experimental parameters on the App and sent them to the detector. According to the command, the detector applied the specific excitation signals on the sensor and recorded the electrochemical responses. The smartphone received the data and plotted it on the screen in real time.

We also developed a WaterSafe central website on the Alibaba Cloud Platform, which could provide the data storage and mapping services. The sample-related information, including the measurement results, dates, and geographical locations, can be sent to the Cloud server through 3G or 4G networks. The submitted data was stored in the SQLite 3 database management system for further analysis. Subsequently, the data points were marked on the website using internet mapping services provided by the Baidu Maps Platform (http://39.108.7.235:5000/Map). The Cloud service is free for all registered users, and we encourage the public to build up the WaterSafe map worldwide.
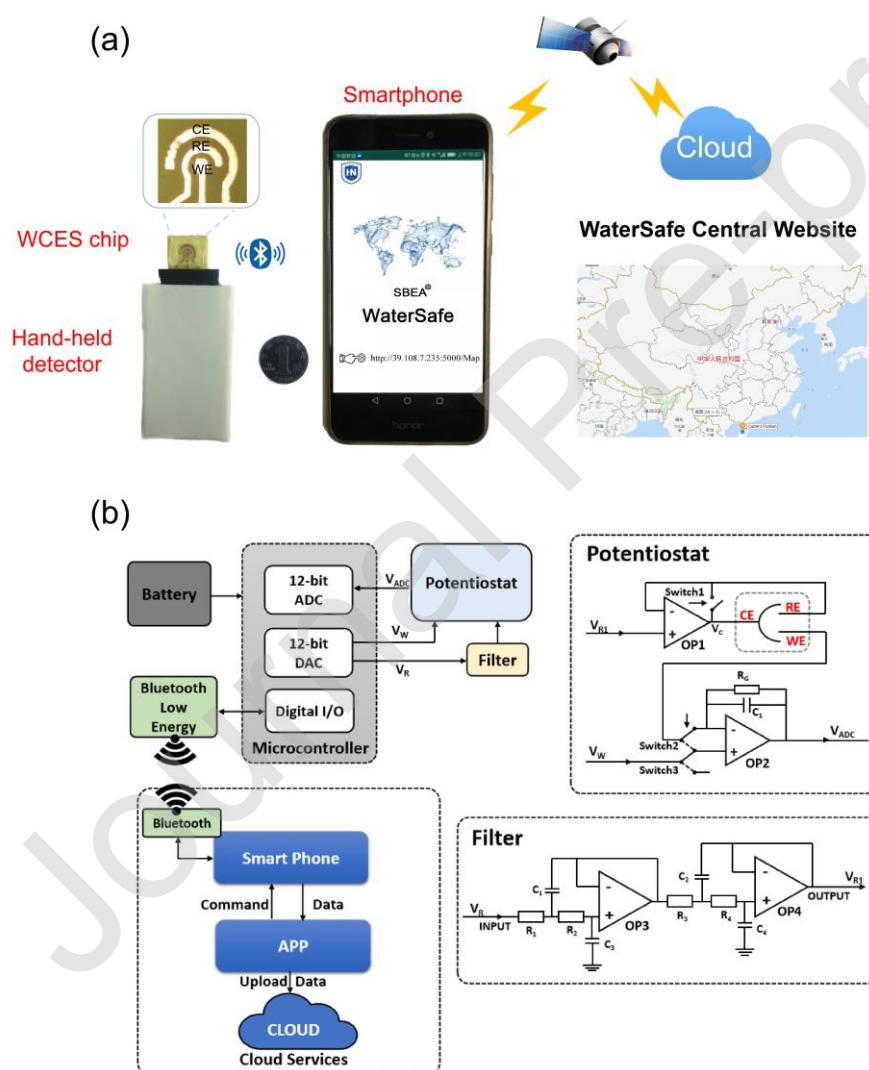

Figure 1. (a) Photograph and (b) schematic diagram of smartphone-based water quality monitoring system, which consists of a WCES chip, a hand-held detector, a

smartphone, and a WaterSafe central website. Working electrode: WE; Counter electrode: CE; Reference electrode: RE.

2.5 Electrochemical measurements

A 100 μL water sample was added into the PDMS well of a WCES chip, and the measurements were conducted after 30 s. For Pb^{2+} detection, the CA and SWV techniques were applied in sequence. First, the CA was carried out at the potential of -0.8 V for 300 s. Second, the SWV was performed as follows: frequency, 15 Hz; amplitude, 25 mV; step potential, 4 mV. For COD detection, the LSV was performed from 0 V to 0.7 V at a scan rate of 0.02 V/s. In order to evaluate the accuracy of the developed system, the same electrochemical experiments were also conducted on a commercial electrochemical analyzer (CHI660E, Shanghai ChenHua Instruments Co., China).

3. Results and discussion

3.1 Evaluation of SBEA

In order to evaluate the accuracy of the SBEA, a redox couple of 5 mM $[Fe(CN)_6]^{3-/4-}$ was used as the electrolyte, and the separated electrodes, including the gold electrode, Ag/AgCl electrode, and platinum electrode, were used as WE, RE, and CE, respectively. As shown in Figure 2, the CV, SWV, and CA curves were almost the same as those of the electrochemical workstation (CHI660E), indicating that SBEA could perform accurate electrochemical measurements. The LSV curve was not shown in Figure 2 because LSV technique is essentially a portion of CV technique. LSV performs only a single scanning from the low potential to the high potential, while CV performs several cyclical scanning from the initial potential to the final potential.
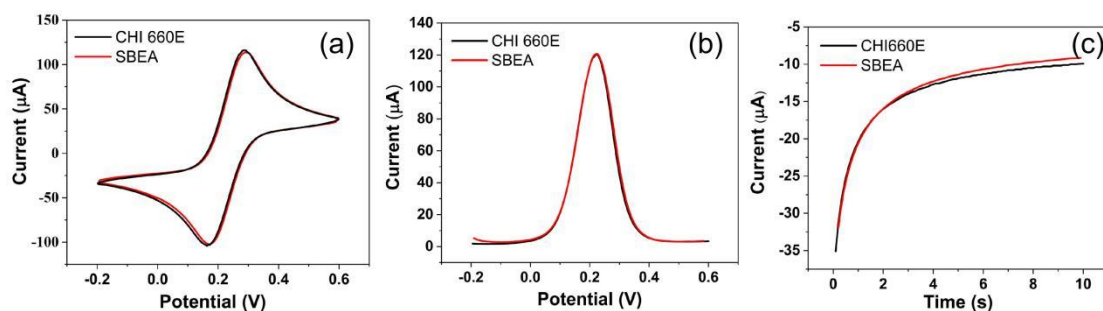
9

Figure 2. Comparison of (a) CV, (b) SWV and (c) CA responses in 5 mM $[Fe(CN)_6]^{3-/4-}$ using SBEA and the commercial electrochemical workstation (CHI660E).

3.2 Evaluation of the WCES chips

3.2.1 Evaluation of Cu WE

As shown in Figure 3a, SWV responses of glassy carbon electrode (GCE), Au, and Cu WEs were compared in 0.1 M acetate buffer containing 10 μM Pb^{2+}. GCE and Au showed stripping potentials at -0.55 V and -0.1 V, respectively, and their corresponding peak currents were 27.8 μA and 8.0 μA, respectively. While for Cu WE, the stripping potential was located at -0.37 V, and the peak current was about 7.0 μA. It can be seen that the different stripping peak potentials and currents were related to the WE material constituents, and thus Cu could be used as the working electrodes.

LSV responses of Cu, Au, Pt, and Ti WEs were also compared in 0.05 M NaOH containing 1 mM glucose. As shown in Figure 3b, when the potential was scanned from 0 V to 0.7 V, the oxidation currents at 0.7 V followed the sequence: Cu > Au > Pt > Ti. There was no electrochemical behavior of glucose at Ti because of its chemical inertness. Pt and Au are two commonly used electrocatalytic materials, and thus showed strong catalytic activities toward glucose. As discussed in Section 3.3.3, Cu(III) species would be generated in an alkaline medium, which can rapidly oxidize organic compounds. Thus, the largest oxidation current was observed on Cu WE.
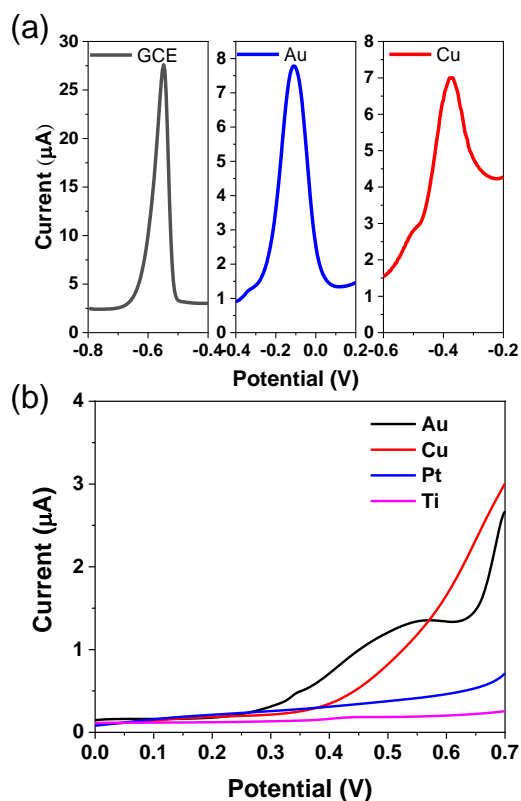
10

Figure 3. (a) SWV responses of 10 μM Pb^{2+} at Cu, Au, and GCE WEs in 0.1 M acetate buffer (pH=5); (b) LSV responses of 1 mM glucose at Cu, Au, Pt and Ti WEs in 0.05 M NaOH (pH=10).

3.2.2 Evaluation of Cu CE

Pt is a commonly used CE material in the conventional three-electrode system. Thus, the stability of Cu CE was evaluated by comparing it with Pt electrode using chronopotentiometry in the acidic and alkaline medium, respectively. During the measurements, a graphite electrode was used as the cathode, Pt and Cu were used as the anodes, and the current was set to be 10 μA.

As shown in Figure 4a, Pt and Cu held stable potentials at 1.3 V and 0.4 V in 0.1 M acetate buffer, respectively. Pt is an excellent polarizable electrode. The potential of water electrolysis was about 1.3 V, and then a stable potential was observed. However, Cu is a typically nonpolarizable electrode. The potential of 0.4 V is not large enough for water electrolysis. To sustain the constant current (10 μA), Cu CE should be oxidized during the testing. The oxidation of Cu could be confirmed by the images

11

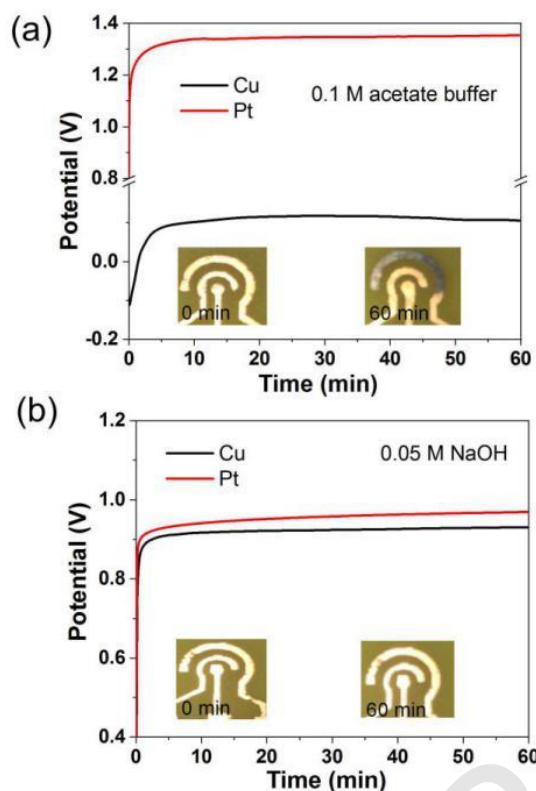shown in the inset of Figure 4a, the color of the Cu electrode has been changed into the dark after 60 min.

Figure 4. Chronopotentiometry of Pt and Cu CEs under the current of 10 µA in (a) 0.1 M acetate buffer (pH = 5) and (b) 0.05 M NaOH (pH = 10) solution, respectively. The insets show the Cu CE images before and after the experiments.

Different results were observed when the supporting electrolyte was replaced with 0.05 M NaOH. The alkaline medium increased the polarization potential of Cu to 0.92 V, while decreased the polarization potential of Pt to 0.96 V. Almost identical polarization potential indicated that the water electrolysis reaction could be sustained on the surface of Pt and Cu in alkaline medium. This speculation was verified by the inset of Figure 4b, where the color of the Cu electrode remained unchanged after 60 min.

For most of electroanalytical techniques, 10 min is long enough for a complete electrochemical measurement. Cu CE could provide acceptable stability within 60

min. Therefore, WCES chips are an attractive option for disposable applications.

3.2.3 Evaluation of Cu/CuCl$_2$ RE

The drift in the potential of the reference electrodes may cause inaccurate measurements. Therefore, it is necessary to evaluate the stability of Cu/CuCl$_2$ RE in both acidic and alkaline medium. As shown in Figures 5a and b, the drift was examined by monitoring the open circuit potential (OCP) against a commercial Ag/AgCl RE. As seen, Cu/CuCl$_2$ RE reached a stable potential after 30 min in 0.1 M acetate buffer, and the potential fluctuation was about 1.0 mV. While Cu/CuCl$_2$ RE showed stability in 0.05 M NaOH from the beginning of the measurements and exhibited a large potential fluctuation of 150 mV. The difference in equilibrium time and potential drift may be due to the different solubility of CuCl$_2$ in the acidic and alkaline media. When the pH of the supporting electrolyte was larger than 7, Cu^{2+} can easily combine with OH$^-$ to form Cu(OH)$_2$ precipitation. Thus a large potential drift was observed in the alkaline medium. We also tested the accelerated electrode aging in a saturated KCl solution (Figure 5c). The potential became steady after 10 min, and the drift rate was 0.26 mV/min, which was much larger than the reported Ag/AgCl RE (~0.005 mV/min) [40,41].

Altogether, although Cu/CuCl$_2$ RE is not a commonly used reference electrode and it shows a significant potential drift in acidic and alkaline media, it is acceptable that the current, but not the potential, is used as the analytical signal in our work. Furthermore, in terms of the simple fabrication procedure and low-cost Cu material, Cu/CuCl$_2$ RE can be used in disposable sensors.
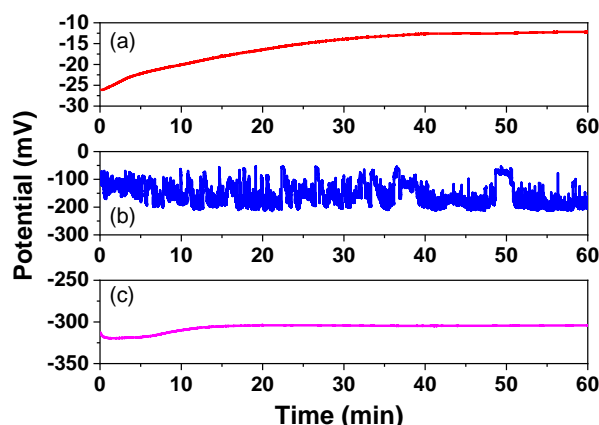
13

Figure 5. Stability of Cu/CuCl$_2$ reference electrode: the open circuit potential of Cu/CuCl$_2$ electrode in (a) 0.1 M acetate buffer (pH=5), (b) 0.05 M NaOH (pH=10), and (c) saturated KCl solution (pH=7).

3.3 Water analysis using the smartphone-based system

3.3.1 Feasibility studies

Sections 3.1 and 3.2 evaluated the performance of SBEA and WCES chips when used individually. Furthermore, we demonstrated the feasibility of smartphone-based water quality monitoring system when they were used in conjunction (Figure S2). In order to enhance the sensitivity and selectivity of smartphone-based system, Cu nanoflowers were electrodeposited onto the Cu WE. Figure S2b shows the SEM image of nano-Cu WE. The Cu nanoflower was composed of nanoparticles with a diameter of 100-200 nm. The XRD patterns (Figure S2c) also indicated that the Cu nanoflowers were pure without the presence of copper oxide.

Figures S2d and e compared the SWV and LSV responses of smartphone-based system with the commercial electrochemical workstation (CHI 660E). For SWV response, a WCES chip and 0.1 M acetate buffer containing 10 μM Pb^{2+} were used. As shown in Figure S2d, the peak current, peak potential, and full width at half maximum of the pulse obtained by the smartphone-based system were almost the same as those obtained by CHI 660E under the same experimental conditions. For LSV response, the same WCES chip and 0.05 M NaOH solution containing 1 mM

14

glucose were used. As the potential scanned from 0 V to 0.7 V, the curve obtained by the smartphone-based system almost coincided with that obtained by CHI 660E (Figure S2e). These results verified that the smartphone-based system could be used as a water quality monitoring platform.

3.3.2 Determination of Pb^{2+} in water

SWV technique has been considered as a promising approach for the determination of heavy metals ions. Our previous work also studied this method in detail, which includes two steps (Figure 6a) [39,42]: i) Preconcentration step. Metal ions are absorbed onto the electrode surface and reduced to atoms when the potential is held at a deposition region ($Pb^{2+} \rightarrow Pb^0$), which can be finished by CA technique in our system. ii) Stripping step. The deposited atoms are oxidized back to metal ions and provide a stripping peak current for the quantification ($Pb^0 \rightarrow Pb^{2+}$), which can be finished by SWV technique in our system.
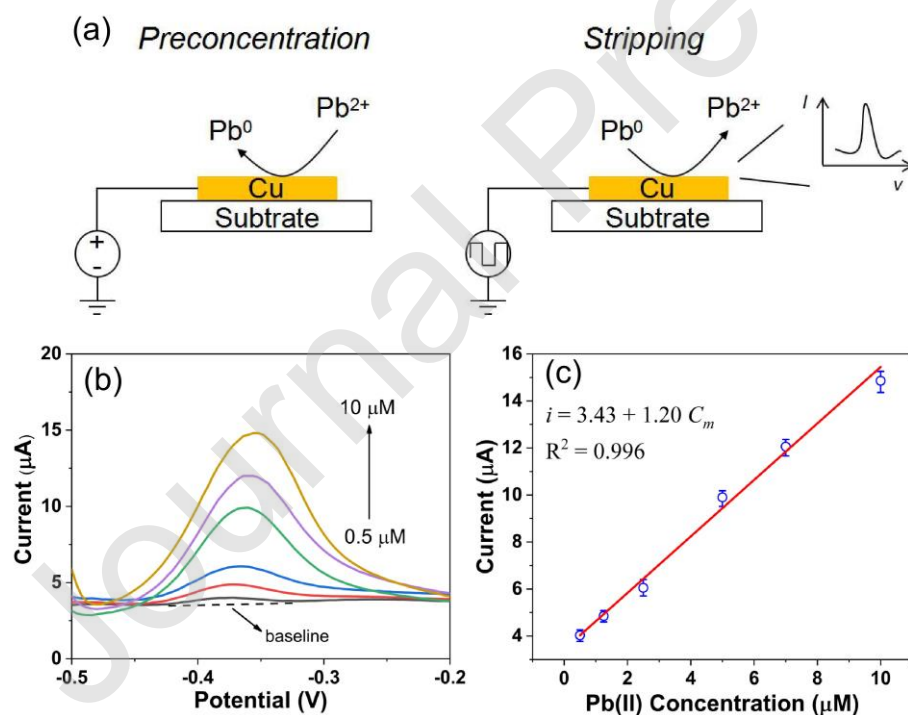

Figure 6. (a) Schematic diagram of SWV technique for the Pb^{2+} detection. (b) SWV responses of the smartphone-based system toward the increasing Pb^{2+} concentrations in 0.1 M acetate buffer (pH=5). (c) The corresponding linear calibration plot of peak

15

currents against Pb^{2+} concentrations.

As shown in Figure 6b, the stripping currents increased with the increase in the concentrations of Pb^{2+} from 0.5 μM to 10 μM. There was a stripping peak around -0.37 V, which was the characteristic of $Pb^0 \rightarrow Pb^{2+}$. The linear equation was:

$$i = 3.43 + 1.20\ C_m,\ R^2 = 0.996 \tag{1}$$
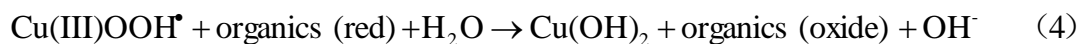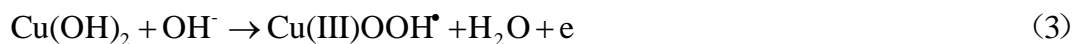
where i is the peak current, and C_m is the mole concentration of Pb^{2+}. The detection limit was estimated to be 45 nM (3δ/slope method), which was comparable to that of the whole-copper sensors (21 nM) reported by Kang et al.[23] However, in Kang's work, deoxygenating water was used for the determination of Pb^{2+}. Because the deoxygenation process is time-consuming and inconvenient, the modification of Cu WE with Cu nanoflowers are used to increase the sensitivity and detection limit in our work, which has been demonstrated to be more straightforward and more effective [43,44].

Cd^{2+} and Zn^{2+} are the potential interference for the SWV determination of Pb^{2+} because the positions of their stripping peaks are close to that of Pb^{2+}. Therefore, the selectivity was studied by detecting 5 μM Pb^{2+} in the presence of Cd^{2+} and Zn^{2+}. If the signal change exceeds 10% relative error, it is considered that the added foreign ion is interference. The results indicated that Cd^{2+} had little effect on the determination of Pb^{2+}. When an equimolar concentration of Cd^{2+} was added, the change of stripping current was 8.6%. The interference caused by Zn^{2+} is insignificant. When the equimolar concentration of Zn^{2+} was added, the change in stripping current was 12.9%. In order to reduce the interference, it is advised to dilute the water samples with acetate buffer solution or add a certain amount of EDTA before the electrochemical measurements [45,46].

3.3.3 Determination of COD in water

LSV was used to analyze the COD level in this work. This technique is based on the measurements of oxidation current of organic compounds on WCES chips. When

the potential is scanned from low to high, metallic copper can rapidly oxidize organic compounds (e.g., glucose) in alkaline media, and the oxidization current is proportional to the concentration of organic compounds in the sample solution. The electrocatalytic oxidation behavior can be expressed as follows [35,47]:

$$Cu + 2OH^- \rightarrow Cu(OH)_2 + 2e \qquad (2)$$

$$Cu(OH)_2 + OH^- \rightarrow Cu(III)OOH^\bullet + H_2O + e \qquad (3)$$

$$Cu(III)OOH^\bullet + organics\ (red) + H_2O \rightarrow Cu(OH)_2 + organics\ (oxide) + OH^- \qquad (4)$$

As observed in Eq (4), Cu(III) is an essential species for the electrocatalytic oxidation of organic compounds, and the demonstration of Cu(III) generated on the surface of the Cu electrode could be found in Figure S3. Furthermore, glucose (Glu), glutaric acid (GA), malonic acid (MA), and potassium hydrogen phthalate (KHP) were selected as model compounds to investigate the COD sensing performance. As shown in Figure S6, when organic compounds were added, the oxidation current increased with the increase of scanning potential, and the currents at 0.7 V followed the order: I(Glu) > I(KHP) > I(MA, GA). The current difference can be explained from the molecular structure and electron transfer number of organic compounds (Table S1).
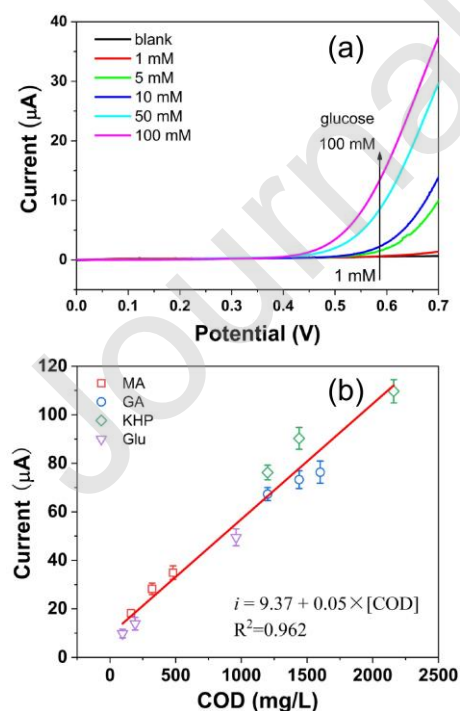
Figure 7. (a) LSV curves of the smartphone-based system in 0.05 M NaOH containing different concentrations of glucose. (b) The relationship between oxidation currents and the theoretical COD values of Glu, GA, MA and KHP.

Figure 7a shows the LSV responses of the smartphone-based system in 0.05 M NaOH containing different concentrations of glucose. The oxidation currents at 0.7 V increased with the concentrations of glucose from 1 mM to 100 mM. KHP, MA, and GA were also tested and showed a similar phenomenon (not shown here). Furthermore, the mole concentration can be converted into the COD concentration using:

$$[COD]=8000n \cdot C_m \tag{5}$$

where n and C_m are the electron transfer number and molar concentration of individual organic compounds, respectively. The relationship between the oxidation currents and theoretical COD values of different organic compounds was depicted in Figure 7b. It was found that the oxidation currents increased linearly with the COD values in the range from 96 mg/L to 2160 mg/L. The linear regression equation was:

$$i = 9.37 + 0.05 \times [COD], R^2 = 0.962 \tag{6}$$

where i is the oxidation current, and [COD] is the COD concentration of organic compounds. The detection limit was estimated to be 9 mg/L (3δ/slope method).

Since chloride ions are the major source of interference in the conventional dichromate method, the effect of chloride ions on the COD determination by the smartphone-based system was investigated. It was found that within the concentration range of Cl$^-$ from 0 to 200 mM, the oxidation current of 1 mM glucose (192 mg/L COD) remained virtually unchanged (signal changes below 10%), illustrating a high tolerance level to the chloride ion.

3.4 Analysis and mapping of the real water samples

In order to assess the practical application of the smartphone-based water quality monitoring system, the detection of Pb^{2+} and COD in real water samples was

18

performed using the standard addition method. The real samples were acquired from Binya Lake, Haikou city, China. Before measurements, the samples were diluted 2X with 0.1 M acetate buffer for the detection of Pb^{2+}, and diluted 2X with 0.05 M NaOH for the detection of COD. Table 1 summarizes the results of Pb^{2+} and COD determination in real samples from nature. The recovery was 97.4% and 103.8% for the Pb^{2+} and COD determination, respectively, indicating the reliability of the developed system.

Moreover, the detection results tagged with the dates and GPS coordinates of the testing sites could be uploaded to the Cloud server, WaterSafe Center Website, for public sharing and viewing. Figure 8 shows the spatiotemporal mapping of Pb^{2+} and COD on the website interfaced with Baidu Maps Platform. The green and red symbols indicated that the sample concentrations were lower and higher than the user-defined threshold values, respectively. Some synthetic data was also added into the database for the real-life situation simulation. As shown in the inset of Figure 8, the user can also review the level of water quality as a function of time for a specific location using a web-based visualization framework [48].
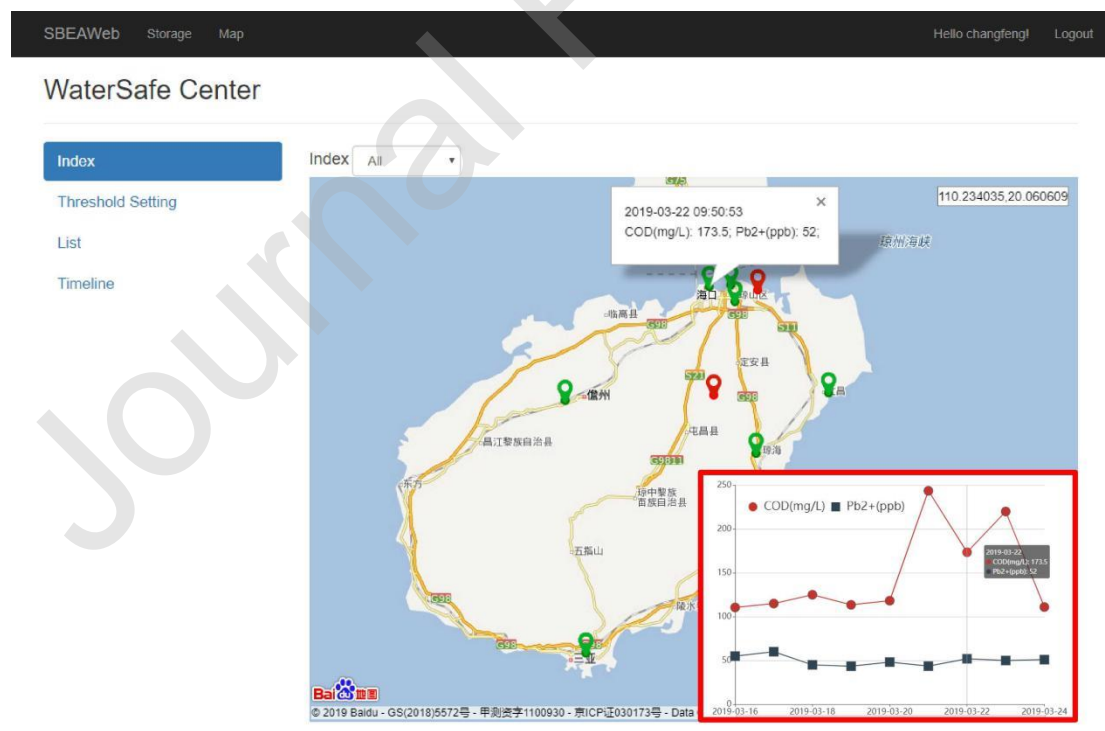

Figure 8. Spatiotemporal mapping of water quality on the website interfaced with

19

Baidu Maps Platform. The green and red symbols indicate that the sample concentrations are lower and higher than the user-defined threshold values, respectively. Inset shows the tracking of water quality as a function of time on a specific location.

3.5 Performance comparison of the smartphone-based system

The smartphone-based water quality monitoring system is composed of four main parts: (i) a WCES chip, (ii) a hand-held detector, (iii) a smartphone equipped with an application program, and (iv) a Cloud map website. First, we compared the Pb^{2+} and COD sensing performance of WCES chips with the previously reported electrochemical sensors (Tables S2 and S3). The linear range and detection limit of the WCES chips are comparable with the previously reported electrochemical sensors. However, the cost has been dramatically reduced because of the low-cost copper and the adopted high-efficiency manufacturing technique. Besides, two water quality indices (Pb^{2+} and COD) could be detected by choosing the acidic or alkaline medium as the supporting electrolyte. Second, the hand-held detector is essentially a mini electrochemical workstation. Four types of electroanalytical techniques (chronoamperometry, cyclic voltammetry, linear sweep voltammetry, and square wave voltammetry) could be accurately performed, and the detector weighs only 50 g, so it is convenient to conduct water quality monitoring in the field. Third, the smartphone is the most widely used mobile device in the world. Thus, the utilization of the smartphone is beneficial for the construction of the water quality contamination map around the world. Finally, a Cloud map website is designed to receive the measured results from the smartphone via 3G or 4G networks, and display the contamination concentration and geographic location in real time. Based on these advantages, a smartphone-based water quality monitoring system may show great potential for the applications in resource-limited settings.

4. Conclusions

We presented a smartphone-based water quality monitoring system, which was

composed of (i) a whole-copper electrochemical sensor, (ii) a hand-held detector, (iii) a smartphone installed with a custom application program, and (iv) a Cloud map website. The smartphone-based system could detect Pb^{2+} and COD in water as low as 45 nM and 9 mg/L, respectively. Moreover, the system could generate a spatiotemporal water quality contamination map based on the Baidu Maps Platform. The cost-effective, field-portable, and wireless-connected system could be rather useful in detecting, tracking, and locating water pollution.

Conflict of Interest Statement

We declare that we have no financial and personal relationships with other people or organizations that can inappropriately influence our work, there is no professional or other personal interest of any nature or kind in any product, service and/or company that could be construed as influencing the position presented in, or the review of, the manuscript entitled, "Wireless water quality monitoring and spatial mapping with disposable whole-copper electrochemical sensors and a smartphone".

Acknowledgment

Reference

[1] J.-M. Jian, Y.-Y. Liu, e.-L. Zhang, X.-S. Guo, Q. Cai, Fast and Sensitive Detection of Pb^{2+} in Foods Using Disposable Screen-Printed Electrode Modified by Reduced Graphene Oxide, *Sensors* 13(2013) 13063-13075.

[2] P.-H. Li, Y.-X. Li, S.-H. Chen, S.-S. Li, M. Jiang, Z. Guo, et al., Sensitive and interference-free electrochemical determination of Pb(II) in wastewater using porous Ce-Zr oxide nanospheres, *Sens. Actuators, B* 257(2018) 1009-1020.

[3] R. Bogdanowicz, J. Czupryniak, M. Gnyba, J. Ryl, T. Ossowski, M. Sobaszek, et al., Amperometric sensing of chemical oxygen demand at glassy carbon and silicon electrodes modified with boron-doped diamond, *Sens. Actuators, B* 189(2013) 30-36.

[4] J. Li, G. Luo, L. He, J. Xu, J. Lyu, Analytical approaches for determining chemical oxygen demand in water bodies: A review, *Crit. Rev. Anal. Chem.* 48(2017) 47-65.

[5] P. Westbroek, E. Temmerman, In line measurement of chemical oxygen demand by means of multipulse amperometry at a rotating Pt ring-Pt/PbO_2 disc electrode, *Anal. Chim. Acta* 437(2001) 95-105.

[6] S. Zhang, D. Jiang, H. Zhao, Development of Chemical Oxygen Demand On-Line Monitoring System Based on a Photoelectrochemical Degradation Principle, *Environ. Sci. Technol.* 40(2006) 2363-2368.

[7] M. Kolb, M. Bahadir, B. Teichgräber, Determination of chemical oxygen demand (COD) using an alternative wet chemical method free of mercury and dichromate, *Water Res.* 122(2017) 645-654.

[8] R.B. Geerdink, R. Sebastiaan van den Hurk, O.J. Epema, Chemical oxygen demand: Historical perspectives and future challenges, *Anal. Chim. Acta* 961(2017) 1-11.

[9] J. Kooistra, Global mobile martket report, Newzoo2018.

[10] J. Shin, S. Chakravarty, W. Choi, K. Lee, D. Han, H. Hwang, et al., Mobile diagnostics: next-generation technologies for in vitro diagnostics, *Analyst* 143(2018) 1515-1525.

[11] S. Kanchi, M.I. Sabela, P.S. Mdluli, Inamuddin, K. Bisetty, Smartphone based

bioanalytical and diagnosis applications: A review, *Biosens. Bioelectron.* 102(2018)
136-149.

[12] D. Quesada-González, A. Merkoçi, Mobile phone-based biosensing: An
emerging "diagnostic and communication" technology, *Biosens. Bioelectron.* 92(2017)
549-562.

[13] I. Hernández-Neuta, F. Neumann, J. Brightmeyer, T. Ba Tis, N. Madaboosi, Q.
Wei, et al., Smartphone-based clinical diagnostics: towards democratization of
evidence-based health care, *J. Intern. Med.* 0(2018).

[14] K. Yang, H. Peretz-Soroka, Y. Liu, F. Lin, Novel developments in mobile sensing
based on the integration of microfluidic devices and smartphones, *Lab on a Chip*
16(2016) 943-958.

[15] A. Roda, E. Michelini, M. Zangheri, M. Di Fusco, D. Calabria, P. Simoni,
Smartphone-based biosensors: A critical review and perspectives, TrAC, *Trends Anal.*
Chem. 79(2016) 317-325.

[16] A. Ainla, M.P.S. Mousavi, M.-N. Tsaloglou, J. Redston, J.G. Bell, M.T.
Fernández-Abedul, et al., Open-Source Potentiostat for Wireless Electrochemical
Detection with Smartphones, *Anal. Chem.* 90(2018) 6240-6246.

[17] J. Guo, Smartphone-Powered Electrochemical Dongle for Point-of-Care
Monitoring of Blood β-Ketone, *Anal. Chem.* 89(2017) 8609-13.

[18] D. Ji, L. Liu, S. Li, C. Chen, Y. Lu, J. Wu, et al., Smartphone-based cyclic
voltammetry system with graphene modified screen printed electrodes for glucose
detection, *Biosens. Bioelectron.* 98(2017) 449-456.

[19] D. Ji, Z. Liu, L. Liu, S.S. Low, Y. Lu, X. Yu, et al., Smartphone-based integrated
voltammetry system for simultaneous detection of ascorbic acid, dopamine, and uric
acid with graphene and gold nanoparticles modified screen-printed electrodes,
Biosens. Bioelectron. 119(2018) 55-62.

[20] D. Ji, N. Xu, Z. Liu, Z. Shi, S.S. Low, J. Liu, et al., Smartphone-based
differential pulse amperometry system for real-time monitoring of levodopa with
carbon nanotubes and gold nanoparticles modified screen-printing electrodes, *Biosens.*
Bioelectron. 129(2018) 216-223.

[21] X. Wang, M.R. Gartia, J. Jiang, T.-W. Chang, J. Qian, Y. Liu, et al., Audio jack based miniaturized mobile phone electrochemical sensing platform, *Sens. Actuators, B* 209(2015) 677-685.

[22] W. Kang, X. Pei, A. Bange, E.N. Haynes, W.R. Heineman, I. Papautsky, Copper-Based Electrochemical Sensor with Palladium Electrode for Cathodic Stripping Voltammetry of Manganese, *Anal. Chem.* 86(2014) 12070-12077.

[23] W. Kang, X. Pei, C.A. Rusinek, A. Bange, E.N. Haynes, W.R. Heineman, et al., Determination of Lead with a Copper-Based Electrochemical Sensor, *Anal. Chem.* 89(2017) 3345-3452.

[24] X. Pei, W. Kang, W. Yue, A. Bange, W.R. Heineman, I. Papautsky, Disposable Copper-Based Electrochemical Sensor for Anodic Stripping Voltammetry, *Anal. Chem.* 86(2014) 4893-4900.

[25] J. Wang, Real-Time Electrochemical Monitoring: Toward Green Analytical Chemistry, *Acc. Chem. Res.* 35(2002) 811-816.

[26] J. Wang, Electrochemical detection for microscale analytical systems: a review, *Talanta* 56(2002) 223-231.

[27] S. Schumacher, J. Nestler, T. Otto, M. Wegener, E. Ehrentreich-Forster, D. Michel, et al., Highly-integrated lab-on-chip system for point-of-care multiparameter analysis, *Lab on a Chip* 12(2012) 464-473.

[28] H.R. Nejad, A. Sadeqi, G. Kiaee, S. Sonkusale, Low-cost and cleanroom-free fabrication of microneedles, *Microsyst. Nanoeng.* 4(2018) 17073.

[29] B. Khadro, A. Sikora, A.S. Loir, A. Errachid, F. Garrelie, C. Donnet, et al., Electrochemical performances of B doped and undoped diamond-like carbon (DLC) films deposited by femtosecond pulsed laser ablation for heavy metal detection using square wave anodic stripping voltammetric (SWASV) technique, *Sens. Actuators, B* 155(2011) 120-125.

[30] L. Zhu, L. Xu, B. Huang, N. Jia, L. Tan, S. Yao, Simultaneous determination of Cd(II) and Pb(II) using square wave anodic stripping voltammetry at a gold nanoparticle-graphene-cysteine composite modified bismuth film electrode, *Electrochim. Acta* 115(2014) 471-477.

[31] S. Zhang, L. Li, H. Zhao, A Portable Photoelectrochemical Probe for Rapid Determination of Chemical Oxygen Demand in Wastewaters, *Environ. Sci. Technol.* 43(2009) 7810-7815.

[32] M. Gutiérrez-Capitán, A. Baldi, R. Gómez, V. García, C. Jiménez-Jorquera, C. Fernández-Sánchez, Electrochemical Nanocomposite-Derived Sensor for the Analysis of Chemical Oxygen Demand in Urban Wastewaters, *Anal. Chem.* 87(2015) 2152-2160.

[33] V. Urbanová, K. Vytřas, A. Kuhn, Macroporous antimony film electrodes for stripping analysis of trace heavy metals, *Electrochem. Commun.* 12(2010) 114-117.

[34] I. Rutyna, M. Korolczuk, Determination of lead and cadmium by anodic stripping voltammetry at bismuth film electrodes following double deposition and stripping steps, *Sens. Actuators, B* 204(2014) 136-141.

[35] C.R. Silva, C.D.C. Conceição, V.G. Bonifácio, O.F. Filho, M.F.S. Teixeira, Determination of the chemical oxygen demand (COD) using a copper electrode: a clean alternative method, *J. Solid State Electrochem.* 13(2009) 665-669.

[36] R. Bogdanowicz, J. Czupryniak, M. Gnyba, J. Ryl, T. Ossowski, M. Sobaszek, et al., Determination of Chemical Oxygen Demand (COD) at Boron-doped Diamond (BDD) Sensor by Means of Amperometric Technique, *Procedia Eng.* 47(2012) 1117-1120.

[37] H. Yu, C. Ma, X. Quan, S. Chen, H. Zhao, Flow Injection Analysis of Chemical Oxygen Demand (COD) by Using a Boron-Doped Diamond (BDD) Electrode, *Environ. Sci. Technol.* 43(2009) 1935-1939.

[38] Q. Cheng, C. Wu, J. Chen, Y. Zhou, K. Wu, Electrochemical Tuning the Activity of Nickel Nanoparticle and Application in Sensitive Detection of Chemical Oxygen Demand, *J. Phys. Chem. C* 115(2011) 22845-22850.

[39] J. Liao, J. Zhang, C.-Z. Wang, S. Lin, Electrochemical and density functional theory investigation on the differential behaviors of core-ring structured $NiCo_2O_4$ nanoplatelets toward heavy metal ions, *Anal. Chim. Acta* 1022(2018) 37-44.

[40] H. Suzuki, H. Shiroishi, S. Sasaki, I. Karube, Microfabricated Liquid Junction Ag/AgCl Reference Electrode and Its Application to a One-Chip Potentiometric

Sensor, *Anal. Chem.* 71(1999) 5069-5075.

[41] B.J. Polk, A. Stelzenmuller, G. Mijares, W. MacCrehan, M. Gaitan, Ag/AgCl microelectrodes with improved stability for microfluidics, *Sens. Actuators, B* 114(2006) 239-247.

[42] J. Liao, F. Yang, C.-Z. Wang, S. Lin, The crystal facet-dependent electrochemical performance of TiO_2 nanocrystals for heavy metal detection: Theoretical prediction and experimental proof, *Sens. Actuators, B* 271(2018) 195-202.

[43] M. Govindhan, B.-R. Adhikari, A. Chen, Nanomaterials-based electrochemical detection of chemical contaminants, *RSC Adv.* 4(2014) 63741-63760.

[44] M. Li, H. Gou, I. Al-Ogaidi, N. Wu, Nanostructured Sensors for Detection of Heavy Metals: A Review, *ACS Sustainable Chem. Eng.* 1(2013) 713-723.

[45] P. Jothimuthu, R.A. Wilson, J. Herren, X. Pei, W. Kang, R. Daniels, et al., Zinc Detection in Serum by Anodic Stripping Voltammetry on Microfabricated Bismuth Electrodes, *Electroanalysis* 25(2013) 401-407.

[46] S. Wu, Q. Zhao, L. Zhou, Z. Zhang, Stripping Analysis of Trace Arsenic Based on the MnO_x/AuNPs Composite Film Modified Electrode in Alkaline Media, *Electroanalysis* 26(2014) 1840-1849.

[47] I.H.A. Badr, H.H. Hassan, E. Hamed, A.M. Abdel-Aziz, Sensitive and Green Method for Determination of Chemical Oxygen Demand Using a Nano-copper Based Electrochemical Sensor, *Electroanalysis* 29(2017) 2401-2409.

[48] D. Li, H. Mei, Y. Shen, S. Su, W. Zhang, J. Wang, et al., ECharts: A declarative framework for rapid construction of web-based visualization, *Vis. Inf.* 2(2018) 136-146.

Author Biographies

Jianjun Liao is an associate professor in the College of Ecology and Environment. His current research interests include chemical sensor and intelligent systems.

Feng Chang is an undergraduate in the College of Applied Science and Technology, Hainan University.

Xiaohu Han is an undergraduate in the College of Applied Science and Technology, Hainan University.

Chengjun Ge is a professor in the College of Ecology and Environment. His current research interests include environmental tonicology & monitoring technology.

Shiwei Lin is a professor in the College of Materials and Chemical Engineering in Hainan University. He received his Phd degree in Electrical and Electronic Engineering from University of Manchester in the U.K. in 2006, Then he conducted two-year postdoctoral research in microelectronics at University of Manchester. His current research interests include solar photocatalysis materials and chemical sensors.

Table 1. Recovery studies of Pb^{2+} and COD determination in real water samples.

Concentration	Added	Found	Detected	Recovery
Pb^{2+} (ppb)	50	52	100.7	97.4%
COD (mg/L)	150	173.5	329.2	103.8%